

# ISLES: Probing Extra Dimensions Using a Superconducting Accelerometer

*Ho Jung Paik, M. Vol Moody, and Violeta A. Prieto-Gortcheva  
Department of Physics, University of Maryland, College Park, MD 20742*

In string theories, extra dimensions must be compactified. The possibility that gravity can have large radii of compactification leads to a violation of the inverse square law at submillimeter distances. The objective of ISLES is to perform a null test of Newton's law in space with a resolution of one part in  $10^5$  or better at  $100 \mu\text{m}$ . The experiment will be cooled to  $\leq 2 \text{ K}$ , which permits superconducting magnetic levitation of the test masses. To minimize Newtonian errors, ISLES employs a near null source, a circular disk of large diameter-to-thickness ratio. Two test masses, also disk-shaped, are suspended on the two sides of the source mass at a nominal distance of  $100 \mu\text{m}$ . The signal is detected by a superconducting differential accelerometer. A ground test apparatus is under construction.

## 1. Objective of ISLES

The Newtonian inverse-square ( $1/r^2$ ) law is a cornerstone of General Relativity. Its validity has been demonstrated to one part in  $10^8$  at  $10^7 \sim 10^9 \text{ km}$  and to one part in  $10^3 \sim 10^4$  at  $1 \text{ cm} \sim 10 \text{ km}$  (Adelberger *et al.*, 1991). The interest in testing Newton's law, at the shortest range possible, has been renewed by a recent suggestion that the  $1/r^2$  law may be violated below  $1 \text{ mm}$  as a manifestation of extra dimensions in spacetime (Arkani-Hamed *et al.*, 1999). The objective of ISLES (Inverse-Square Law Experiment in Space) is to perform a null test of Newton's law in space with a resolution of one part in  $10^5$  or better at ranges between  $100 \mu\text{m}$  to  $1 \text{ mm}$ .

Figure 1 shows the existing limits for the  $1/r^2$  law at ranges below  $1 \text{ mm}$  (Hoyle *et al.*, 2001; Long *et al.*, 2003) and the anticipated sensitivities of ISLES on board the ISS, plus expected sensitivities for its free-flyer and ground versions, plotted as functions of the range  $\lambda$ . The expected resolution of ISLES (at  $2\sigma$ ) on the ISS is  $|\alpha| = 2 \times 10^{-5}$  at  $\lambda = 100 \mu\text{m}$  and  $|\alpha| = 2 \times 10^{-2}$  at  $\lambda = 10 \mu\text{m}$ , where the total potential is written as

$$V(r) = -\frac{GM}{r}(1 + \alpha e^{-r/\lambda}). \quad (1)$$

This resolution represents an improvement over the existing limit at  $\lambda = 100 \mu\text{m}$  by six orders of magnitude. The improvement at shorter ranges is even greater. The free-flyer version improves the resolution by another two orders of magnitude. ISLES is also capable of detecting the axion, a candidate dark-matter particle and will probe the extra dimensions down to a few  $\mu\text{m}$ .

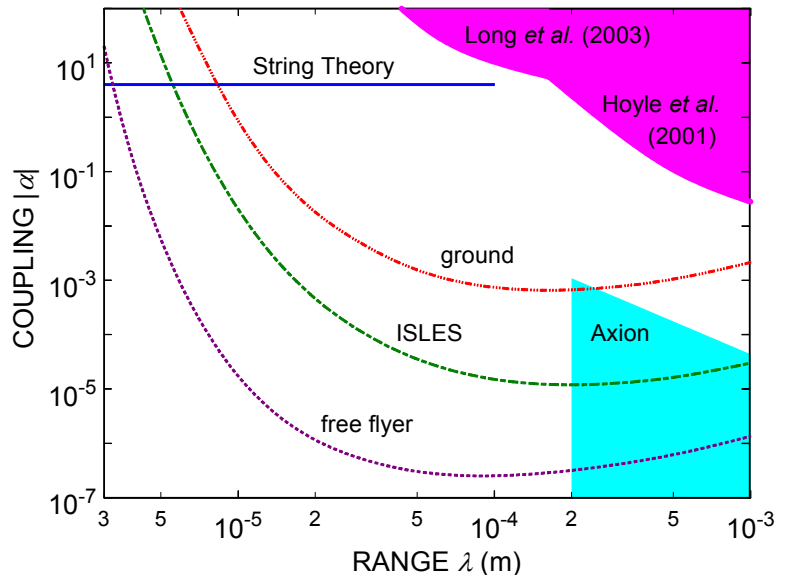


Figure 1. Sensitivity of ISLES versus the existing limit.

## 2. Scientific Value of Short-Range $1/r^2$ Law Test

**Search for extra dimensions.** String theories can be consistently formulated only in nine spatial dimensions. Because the space we observe is three-dimensional, the extra dimensions must be hidden. It is possible to have dimensions that affect gravity but not elementary particles, if elementary particles are localized on a three-dimensional subspace (“brane”) embedded in a higher-dimensional space.

String theory is defined in terms of a fundamental scale  $M_*$ . If there are  $n$  compact dimensions with radii  $R_1, R_2, \dots, R_n$ , Gauss’s law implies that the Planck mass  $M_{Pl}$  is related to  $M_*$  by

$$M_{Pl}^2 \approx M_*^{2+n} R_1 R_2 \dots R_n . \quad (2)$$

As we probe distances shorter than one of the radii  $R_i$ , a new dimension opens up and changes the  $r$  dependence of the gravitational force law.

Cosmological and astrophysical constraints give a bound  $M_* > 100$  TeV (Cullen and Perelstein, 1999; Hall and Smith, 1999), with the most stringent bound,  $M_* > 1700$  TeV, coming from the evolution of neutron stars (Hannestad and Raffelt, 2002). For two large extra dimensions of the same magnitude, this most stringent bound corresponds to  $R_1 \approx R_2 \leq 40$  nm. While this is beyond the reach of our experiment, there are untested cosmological assumptions going into these bounds. Another interesting scenario is the case of two or more large extra dimensions with  $R_1 \gg R_2, \dots, R_n$ . Since Eq. (2) depends only on the product, we can have  $M_* \geq 100$  TeV while still having  $R_1$  near the experimental limit.

Thus new developments in string theories raise the possibility that there may be deviations from Newton’s law between micron and millimeter length scales. These developments represent the first prediction of a string theory that can be tested, and a discovery of such a deviation from the  $1/r^2$  law would be ground breaking. A null result would also be significant in that, in addition to extending the limits of the  $1/r^2$  law and General Relativity, it will put constraints on the string scale and on the sizes of any possible extra dimension.

**Search for the axion.** In strong interactions, non-perturbative effects induce violations of parity ( $P$ ) and charge conjugation-parity ( $CP$ ) symmetries, parameterized by a dimensionless angle  $\theta$ . The *a priori* expectation for the magnitude of  $\theta$  is of the order of unity, but no such violations of  $P$  or  $CP$  have been observed in strong interactions. In particular, present upper bounds on the neutron electric dipole moment (Altarev *et al.*, 1992) require  $\theta \leq 3 \times 10^{-10}$ .

Peccei and Quinn (1977) developed an attractive resolution of this strong  $CP$  problem. One ramification of their theory is the existence of a new light-mass boson, the *axion* (Weinberg, 1978; Wilczek, 1978). The axion mediates a short-range mass-mass interaction. The upper bound  $\theta \leq 3 \times 10^{-10}$  corresponds to a violation of the  $1/r^2$  law at the level of  $|\alpha| \approx 10^{-3}$  at  $\lambda = 200$   $\mu\text{m}$ , which is well within the reach of our experiment.

The axion could also solve the major open question in astrophysics: the composition of dark matter. Although neutrino mass, MACHOs (MASSive Compact Halo Objects), and many hypothetical particles have been offered as explanations, the solution remains elusive. The axion is one of the strongest candidates for the cold dark matter (Turner, 1990). Confirmation (or rejection) of this prediction would therefore have a major impact in our understanding of the universe, from its most microscopic constituents to its grand scale.

### 3. Principle of Experiment

**Newtonian null source.** To maximize the masses that can be brought to within  $100\ \mu\text{m}$  from each other, flat disk geometry is used for both the source and test masses. An infinite plane slab is a Newtonian null source. We approximate this null source of Newtonian gravity by using a circular disk of a sufficiently large diameter-to-thickness ratio. Figure 2 shows the configuration of the source and test masses with associated coils and capacitor plates.

**Levitated test masses.** Two disk-shaped superconducting test masses are suspended on the two sides of the source mass and are coupled magnetically to form a differential accelerometer. The average position of the test masses with respect to the housing are measured with capacitors  $C_1$  and  $C_2$ , while the motions induced in the levitated test masses are detected by sensing coils ( $L_{S1}$  and  $L_{S2}$ ).

In Earth's gravity (1 g), it is difficult to suspend two flat disks on two sides of the source mass at such proximity without significantly modifying the geometry and stiffening the differential mode, thus degrading the resolution of the experiment. In micro-gravity, each test mass can be suspended by applying only minute forces from a pancake coil ( $L_{S1}$  or  $L_{S2}$ ) and a small ring coil ( $L_{R1}$  or  $L_{R2}$ ) coupled to a narrow slanted rim of the test mass.

**Second harmonic detection.** As the source mass is driven at frequency  $f_S$  along the symmetry axis, the first-order Newtonian fields arising from the finite diameter of the source mass are canceled upon differential measurement, leaving only a second-order error at  $2f_S$ . By symmetry, the Yukawa signal of Eq. (1) also appears at  $2f_S$ . The second harmonic detection, combined with the common-mode rejection ratio (CMRR) of the detector, reduces source-detector vibration coupling by over 300 dB.

**Expected signal.** The design allows a source displacement of up to  $\pm 50\ \mu\text{m}$ . The differential acceleration signals expected from the Newtonian force errors (with 90% correction) and from the Yukawa forces with  $|\alpha| = 10^{-5}$  and  $\lambda = 100\ \mu\text{m}$  are plotted in Figure 3 as a function of the source mass position. The rms amplitude of the Yukawa signal, corresponding to a  $\pm 50\text{-}\mu\text{m}$  displacement, is  $8.5 \times 10^{-12}\ \alpha\ \text{m s}^{-2}$ . The rms amplitude of the Newtonian term, arising from the finite diameter of the source mass, is  $1.0 \times 10^{-16}\ \text{m s}^{-2}$  before compensation. The Newtonian error will be computed and removed to  $\leq 10\%$ , which is trivial.

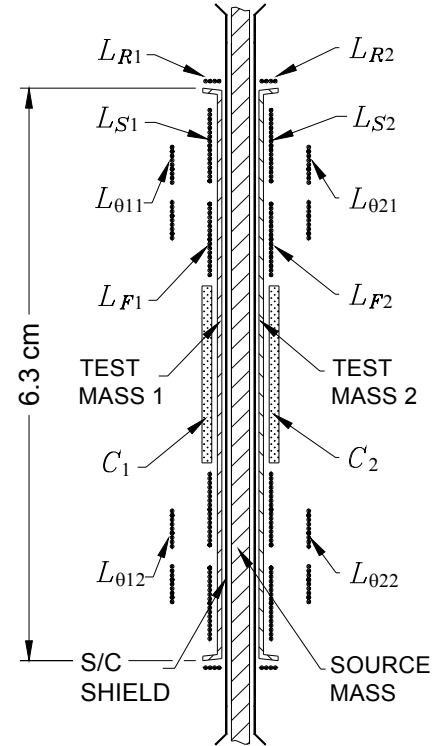


**Figure 2. Configuration of the source and test masses.**

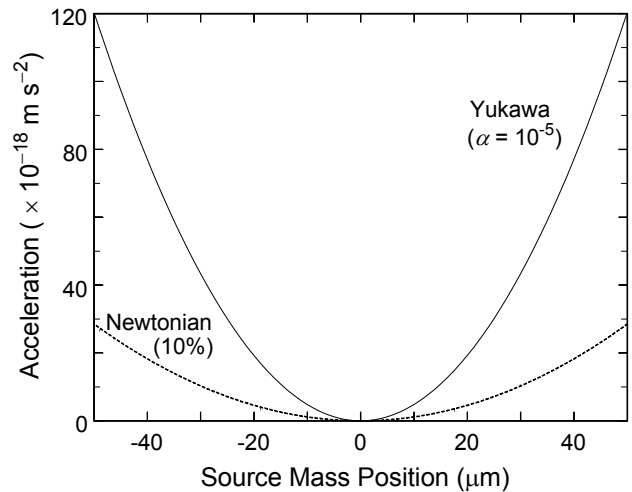


**Figure 3. Newtonian (compensated) and Yukawa signals versus source mass position.**

## 4. Experimental Hardware

**Overview of the apparatus.** Figure 4 shows a cross-sectional view of the apparatus for the ISS experiment. The entire housing is fabricated from niobium (Nb). The source mass is suspended by cantilever springs at the edge and driven magnetically. A thin Nb shield provides electrostatic and magnetic shielding between the source and each test mass. The test masses are suspended and aligned by magnetic fields from various coils. Two auxiliary superconducting accelerometers are mounted on two sides of the housing to provide linear and angular acceleration signals as well as a gravity gradient signal.

The entire assembly weighs 6.0 kg and fits within the 20-cm diameter envelope of the LTMPF instrument well. The apparatus is fastened to the second-stage thermal platform of the Cryo Insert, where the temperature will be stabilized to  $\leq 5 \mu\text{K}$ . The detector orientation is chosen so that its sensitive axis is aligned with the pitch ( $y$ ) axis of the ISS. This orientation minimizes the centrifugal acceleration noise acting on the test masses.

**Source and test masses.** The source mass is a disk 2.0 mm thick by 140 mm in diameter, with mass  $M = 510 \text{ g}$ . The source mass, cantilever springs, and rim are machined out of a single plate of Ta. Ta is chosen for its high density ( $16.6 \text{ g cm}^{-3}$ ) and its relatively high  $H_c$ . Each test mass is a Nb disk 0.25 mm thick by 63 mm in diameter, with a rim 0.25 mm thick by 2.0 mm wide, which has  $5^\circ$  slant from the axis. The mass of each test mass is  $m = 7.5 \text{ g}$ .

**Superconducting circuitry.** Schematics of the superconducting circuits for the detector are shown in Figure 5. These circuits are similar to the standard differencing circuit used at the University of Maryland in the superconducting gravity gradiometer (SGG) (Moody *et al.*, 2002). The test masses are suspended radially by storing persistent currents  $I_{R1}$  and  $I_{R2}$  in ring coils  $L_{R1}$  and  $L_{R2}$ , as shown in Figure 5(a). Due to the slanted rim of the test masses, currents  $I_{R1}$  and  $I_{R2}$  will also exert an axially outward force on the test masses. This outward force is balanced by the axially inward forces provided by the currents in the sensing, alignment, and feedback coils.

The scale factors of the component accelerometers are matched by adjusting currents  $I_{S1}$  and  $I_{S2}$  in pancake coils  $L_{S1}$  and  $L_{S2}$ , shown in Figure 5(b). The SQUID measures the differential acceleration  $a_D$ , or gravity gradient, along the  $y$ -axis. To align an individual test mass parallel to its shield as well as the other test mass, two alignment circuits are provided for each test mass, one per degree of freedom. Figure 5(c) shows the alignment circuit of test mass 1 about the  $x$ -axis. To suppress the nonlinearity of the scale factors, a feedback is applied to the test masses, which *actively* stiffens the modes. The common-mode (CM) and differential-mode (DM) outputs  $i_{FC}$

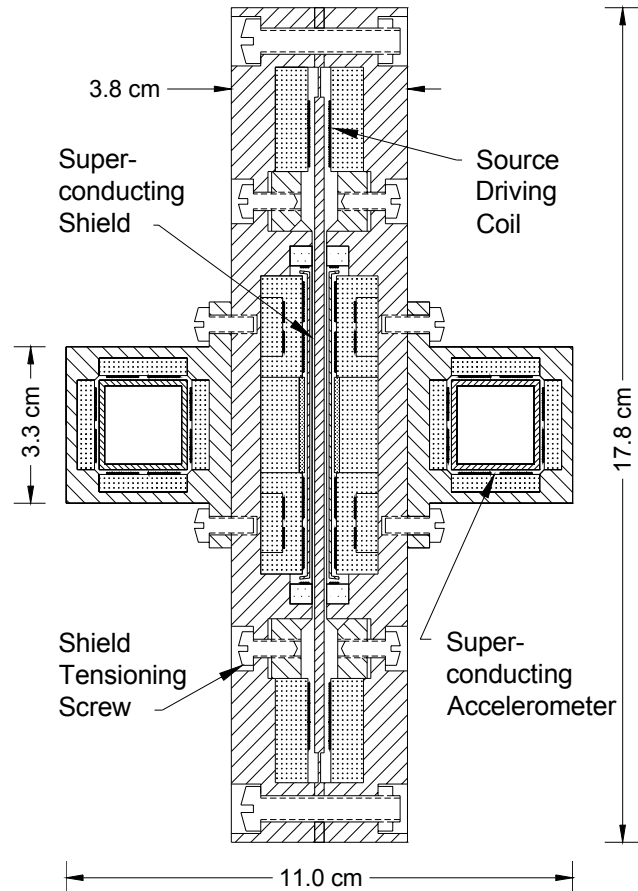
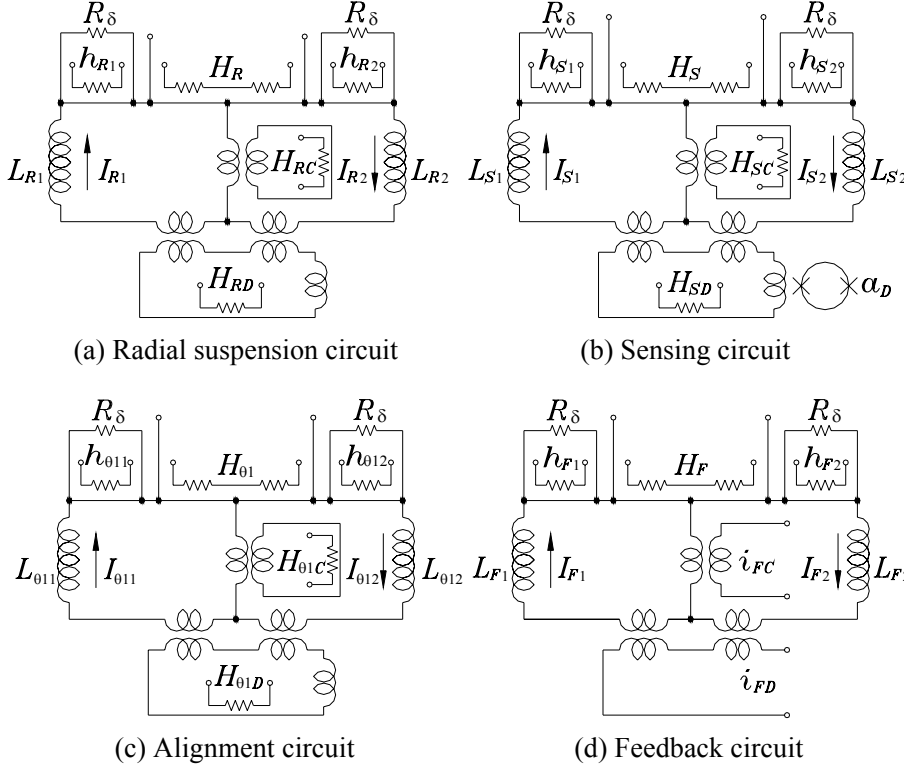


Figure 4. Cross section of the ISLES apparatus.



**Figure 5. Superconducting circuits for the detector.**

resolution, fluxes can then be adjusted in the aligning, suspension, and readout coils to one part in  $10^5$ . This gives the ability to match the scale factors to  $10^{-5}$  and to align the sensitive axes to  $10^{-5}$  rad, resulting in an initial CMRR of  $10^5$  in all three linear degrees of freedom.

**Auxiliary superconducting accelerometers.** Figure 4 shows two three-axis auxiliary superconducting accelerometers mounted symmetrically on the two sides of the instrument housing. Each test mass is a hollow 20-g Nb cube, suspended and sensed by Nb pancake coils on its six faces. The accelerometers are coupled to SQUIDs to measure three linear ( $a_i$ ) and two angular ( $\alpha_i$ ) acceleration components, plus a gravity gradient component ( $\Gamma_{ij}$ ). The unmeasured component  $\alpha_y$  is not needed for error compensation.

**Error compensation.** Linear and angular accelerations are rejected to  $10^{-5}$  and  $10^{-4}$  m, respectively, by adjusting persistent currents in the sensing and alignment circuits. To improve the rejection further, we apply error compensation techniques that have been demonstrated with our SGG (Moody *et al.*, 2002). During the experiment, the linear and angular accelerations of the platform, measured by the auxiliary accelerometers, are multiplied by the predetermined error coefficients (transfer functions) and are subtracted from the detector output. By applying the compensation factor  $10^3$  to the noise levels, demonstrated in the laboratory, the linear and the angular acceleration rejections are improved to  $10^8$  and  $10^{-7}$  m, respectively.

Due to the short but finite baseline ( $\ell \approx 2.5$  mm), the  $1/r^2$  law detector is a gravity gradiometer that is sensitive to attitude modulation of Earth’s gravity gradient, to acceleration noise from ISS, and to centrifugal accelerations. The auxiliary gradiometer measures exactly the same gradient noise, except for gravity disturbances from nearby objects ( $< 1$  m). This noise can thus be removed from the detector output by applying the same correlation method.

and  $i_{FD}$  are fed back to the test masses, as shown in Figure 5(d). The CM output is derived from the auxiliary accelerometers.

**Coarse and fine heat-switches.** To be able to control the magnetic fluxes trapped in various superconducting loops with sufficient precision in the noisy environment of the ISS, two sets of heat-switches are provided: coarse heat-switches,  $H_{ij}$ ’s, with an  $L/R$  time constant of  $\sim 10$  ms, and fine heat-switches,  $h_{ij}$ ’s, with a time constant of  $\sim 100$  s. With 1-ms time

## 5. Error Budget

**Metrology errors.** The effects from the finite diameter of the source and the dynamic mass of the suspension springs are corrected to 10% and 20%, respectively. Linear taper and linear density variation of the source produce second order errors, which become negligible. The test masses tend to rotate slowly about the sensitive axis, averaging out the asymmetry about the axis. Hence only the radial taper and the radial density variation are important. Due to the null nature of the source, test mass metrology is not important, except for the extended rim. The rim dimension is fabricated to 2.5  $\mu\text{m}$  tolerance. The total metrology error is  $1.5 \times 10^{-17} \text{ m s}^{-2}$ .

**Intrinsic instrument noise.** The intrinsic power spectral density of a superconducting differential accelerometer is given (Chan and Paik, 1987; Moody *et al.*, 2002) by

$$S_a(f) = \frac{8}{m} \left[ \frac{k_B T \omega_D}{Q_D} + \frac{\omega_D^2}{2\eta\beta} E_A(f) \right], \quad (3)$$

where  $m$  is the mass of each test mass,  $\omega_D = 2\pi f_D$  and  $Q_D$  are the differential-mode resonance frequency and quality factor for the test mass motions,  $\beta$  is the electromechanical energy coupling coefficient from the test mass motions to the electrical circuits,  $\eta$  is the electrical energy coupling coefficient of the SQUID, and  $E_A(f)$  is the input energy resolution of the SQUID.

Equation (3) shows that  $f_D$  is a critical parameter for the intrinsic noise. The microgravity environment on ISS, in principle, allows a suspension  $10^6$  times softer than on the ground, which corresponds to  $f_D < 0.01$  Hz. On the other hand, the test mass displacement in response to the ISS vibration must be minimized to reduce errors due to electric charge, patch-effect fields, self-gravity of the ISS, and most importantly the nonlinearity of the scale factors. Further, the test mass suspension must be stiff enough to keep the test masses from bumping into the housing before the feedback loop is closed. This requirement leads to  $f_C \geq 0.2$  Hz. Ideally, one would increase  $f_C$  as much as possible, while keeping  $f_D$  low. Unfortunately, the nonlinearity of the coils couples a fraction of the CM stiffness to DM, providing a practical limit:  $f_C/f_D \leq 4$ . Therefore,  $f_C \geq 0.2$  Hz implies  $f_D \geq 0.05$  Hz.

Substituting  $f_D = 0.05$  Hz,  $T = 2$  K,  $m = 7.5$  g,  $Q_D = 10^6$ ,  $\beta = \eta = 0.5$ , and typical SQUID noise  $E_A(f) = 10^{-30} (1 + 0.1 \text{ Hz}/f) \text{ J Hz}^{-1}$ , we find the intrinsic noise of the instrument to be  $S_a^{1/2}(f) = 7.0 \times 10^{-14} \text{ m s}^{-2} \text{ Hz}^{-1/2}$  at  $f = 0.02$  Hz.

**Acceleration Noise.** The  $y$ -axis acceleration measured by a SAMS II accelerometer in the US Lab on a typical day corresponds to  $3 \times 10^{-6} \text{ m s}^{-2} \text{ Hz}^{-1/2}$  at 0.02 Hz. Assuming that the ISLES detector experiences the same acceleration at its position on the ISS, this noise is reduced to  $3 \times 10^{-14} \text{ m s}^{-2} \text{ Hz}^{-1/2}$  by the net CMRR of  $10^8$ . The angular acceleration noise is reduced to  $2 \times 10^{-14} \text{ m s}^{-2} \text{ Hz}^{-1/2}$  by the net error coefficient of  $10^{-7}$  m. The centrifugal acceleration noise is negligible. The nonlinearity noise will be reduced to  $< 10^{-14} \text{ m s}^{-2} \text{ Hz}^{-1/2}$  under a feedback control, which stiffens CM to 10 Hz. The total acceleration noise then becomes  $6.3 \times 10^{-14} \text{ m s}^{-2} \text{ Hz}^{-1/2}$  at  $f = 0.02$  Hz.

**Gravity noise.** Helium tide is absent due to the Earth-fixed orientation of the ISS. Helium sloshing is of minor concern since it is expected to occur at a sufficiently low frequency,  $\sim 2.5$  mHz. The gravity noise from modulation of the Earth's gravity gradient and from ISS self-gravity, including the activities of astronauts, along with the centrifugal acceleration, will be taken out by the error compensation scheme described above.

**Magnetic crosstalk.** Trapped flux is not of concern as long as the flux is strongly pinned. Flux creep will be minimized by cooling and performing the experiment in a low magnetic field. For this purpose, LTMPF is equipped with a Cryoperm magnetic shield.

With the high magnetic field required to drive the source mass, magnetic crosstalk between the source and the detector is a very important potential source of error. To solve this problem, the entire detector housing is machined out of Nb and a thin Nb shield is provided between the source and each test mass. High-purity Nb will be used. The Nb will be heat-treated to bring the material very close to a type-I superconductor, thus minimizing flux penetration. The superconducting shield is expected to provide over 200-dB isolation (Rigby *et al.*, 1990). This shielding, combined with 60-dB rejection from the second harmonic detection, should provide the required isolation between the source drive signal and the test masses in excess of 260 dB.

**Electric charge effects.** Levitated test masses in orbit will accumulate electric charge from cosmic rays and from high-energy protons as the spacecraft traverses through the South Atlantic Anomaly. Scaling from the charge computed for STEP test masses (Blaser *et al.*, 1996) and correcting for differences in test mass shapes, we find the total charge accumulated in each test mass over the duration of the experiment to be  $Q \approx 1.5 \times 10^{-13}$  C.

The charge trapped in the test mass will induce image charges on the neighboring coils and superconducting ground planes. These charges will generate a differential force  $Q^2/\epsilon_0 A$ , where  $\epsilon_0$  is the permittivity of vacuum and  $A$  is the area of the test mass. The force results in the maximum differential displacement at the end of the mission:

$$x_{D,\max} = \frac{Q^2}{\epsilon_0 A} \frac{1}{m\omega_D^2} \approx 7 \times 10^{-9} \text{ m}. \quad (4)$$

This displacement affects the CMRR through mismatches in the accelerometers. With the initial coil gap of  $10^{-4}$  m and a mismatch of 10%, we find that the CMRR is affected by only 7 ppm. This charging-induced error should allow the passive CMRR to remain at the required level of  $10^5$  throughout the mission. So it appears that ISLES does not require a discharging system. We are planning to carry out a more refined analysis of trapped charge for ISLES.

The energetic charged particles will also impart momentum and cause heating of the test masses. For the STEP study, these effects were found to be less important than the electrostatic force. In addition, the patch-effect potential will be modulated as charge builds up in the test masses, causing a time-varying acceleration. These ac disturbances occur mostly outside the signal band and therefore are averaged out. The Casimir force is not of concern for the present experiment where the gap between the masses is  $\geq 10 \mu\text{m}$  (Lamoreaux, 1997).

**Temperature noise.** The modulation of the penetration depth of a superconductor with temperature and residual thermal expansion coefficients of materials give rise to temperature sensitivity in a superconducting accelerometer. These occur through temperature gradients and mismatches in the accelerometers (Chan and Paik, 1987). From our experience with the SGG, however, this noise is expected to be negligible with the temperature stabilized to 5  $\mu\text{K}$ .

**Total errors.** Table 1 combines all the errors for the ISS experiment. To reduce the random noise to the levels listed, a 90-day integration period was assumed. Dominant error sources are the intrinsic noise of the differential accelerometer and the platform noise. These errors can be reduced by at least two orders of magnitude by going to a free-flyer.

## 6. Expected Resolution

By equating the total error with the expected Yukawa signal, we compute the minimum detectable  $|\alpha|$ . Figure 1 shows the  $2\sigma$  errors plotted as a function of  $\lambda$ . The best resolution of ISLES on board ISS is  $|\alpha| = 2 \times 10^{-5}$  at  $\lambda = 100 \mu\text{m} \sim 1 \text{ mm}$ . Extra dimensions will be searched to  $R_2 \geq 5 \mu\text{m}$  and axions with strength 10 - 100 times below the maximum will be detected.

The resolution of the experiment could be improved by reducing several errors. The metrology and density errors could be reduced by fabricating the source mass out of a crystalline material such as sapphire or quartz, which can be optically polished. The masses would then be coated with a thin layer of Nb. The vibration noise can be improved by several orders of magnitude by going to a free-flyer. Lower vibration levels will allow much softer suspension of the test masses and thus will result in higher instrument sensitivity. The quieter platform will also allow a smaller gap between the masses. With these improvements, a free-flyer ISLES is expected to achieve the resolution depicted by the bottom curve in Figure 1. A free-flyer option of ISLES is under investigation.

Figure 1 also shows the expected sensitivity of our ground experiment. Under 1-g, the test masses will be suspended mechanically by cantilever springs similar to the source mass. The resulting stiffness of the DM modes ( $\geq 5 \text{ Hz}$ ) will compromise the resolution of the experiment to  $|\alpha| = 10^{-3}$  at  $\lambda = 100 \mu\text{m}$ . However, this resolution already improves over the existing limit by four orders of magnitude and will be a great stepping stone for a space experiment.

## 7. Ground Test Apparatus

In order to set a milestone for the  $1/r^2$  law test and work out the operational procedures for the orbital experiment, we are constructing a ground test apparatus. Figure 6 is an expanded cross section of the apparatus. A major departure from the space instrument is the mechanical suspension of the test masses.

This ground experiment will provide an opportunity to demonstrate the required scale factor match and axis alignment of the test masses. In addition, the integrity of the superconducting shield and the level of magnetic crosstalk will be investigated. In the process of designing and carrying out error analysis for the ground experiment, we have discovered that the mechanical cross coupling through the source-driven distortion of the housing is a critical error source. To decouple the detector sufficiently from this distortion, we have found it necessary to insert a weak mechanical link between the outer rim, which supports the source mass, and the inner test mass blocks (see Figure 6). This feature will also be incorporated into the design of ISLES instrument.

ISLES will use the SGG technology fully developed at the University of Maryland. The SGG has been used to perform a null test of Newton's law at sensitivity ten times beyond that of the other methods at 1-meter distance (Moody and Paik, 1993). The instrument proposed for ISLES is very similar to the existing SGG. The experimental procedure and error analysis are also similar in many ways to those in the meter-scale  $1/r^2$  law test, already carried out with the

Error Source	Error ( $\times 10^{-18} \text{ m s}^{-2}$ )
Metrology	15
Random	(90 days)
Intrinsic	25
ISS vibration	23
Gravity noise	< 1
Vibration coupling	< 1
Magnetic coupling	< 10
Electric charge	< 10
Other (30% margin)	33
Total	52

**Table 1. Error budget.**

SGG. However, the present short-range experiment is much more sensitive to the density inhomogeneity and dimensional errors of the source mass.

The meter-scale experiment employed a Gaussian null detector (Paik, 1979), which made it relatively insensitive to the source errors. In the present experiment, the source itself must produce a uniform field. The test masses are located so close ( $\sim 100 \mu\text{m}$ )

to the surfaces of the source mass that they will be directly sensitive to the imperfections of the source mass. At present, we are exerting a major effort on understanding and controlling the source metrology errors.

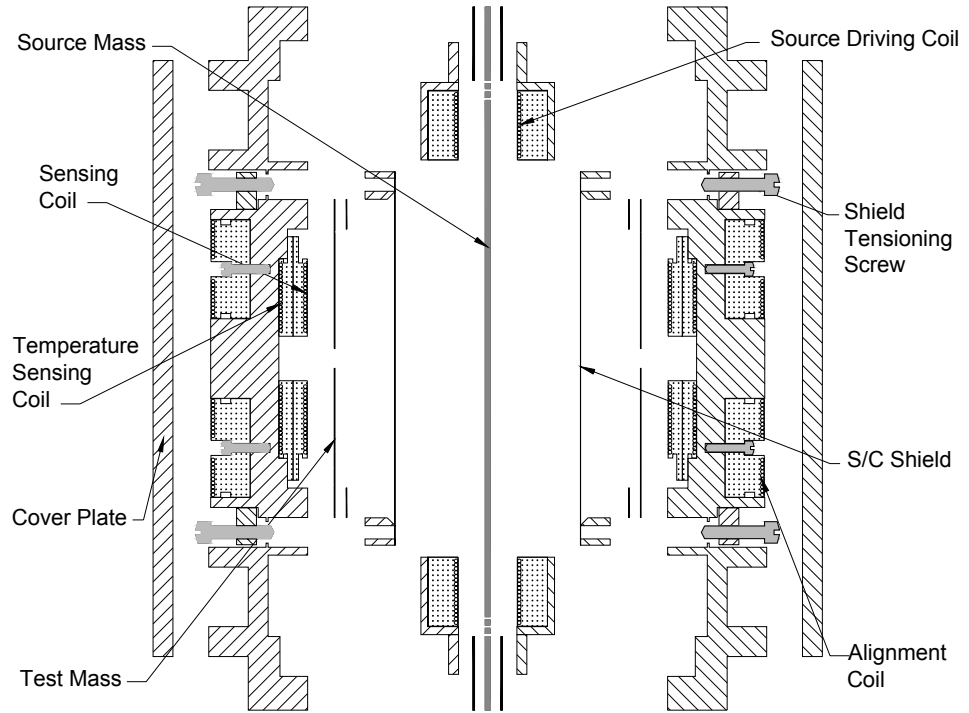


**Figure 6. Expanded cross section of the ground experiment.**

## References

- Adelberger, E. G. *et al.* (1991), *Ann. Rev. Nucl. Part. Sci.* **41**, 269.  
 Altarev, I. S. *et al.* (1992), *Phys. Lett. B* **276**, 242.  
 Arkani-Hamed, N., Dimopoulos, S., and Dvali, G. (1999), *Phys. Rev. D* **59**, 086004.  
 Blaser, J.-P. *et al.* (1996), *STEP*, Report on the Phase A Study, SCI(96)5.  
 Chan, H. A. and Paik, H. J. (1987), *Phys. Rev. D* **35**, 3551.  
 Cullen, S. and Perelstein, M. (1999), preprint hep-ph/9903422.  
 Hall, L. J. and Smith, D. (1999), *Phys. Rev. D* **60**, 085008.  
 Hannestad, S. and Raffelt, G. G. (2002), *Phys. Rev. Lett.* **88**, 071301.  
 Hoyle, C. D. *et al.* (2001), *Phys. Rev. Lett.* **86**, 1418.  
 Lamoreaux, S. K. (1997), *Phys. Rev. Lett.* **78**, 5.  
 Long, J. C. *et al.* (2003), *Nature* **421**, 922.  
 Moody, M. V. and Paik, H. J. (1993), *Phys. Rev. Lett.* **70**, 1195.  
 Moody, M. V., Canavan E. R., and Paik, H. J. (2002), *Rev. Sci. Instrum.* **73**, 3957.  
 Paik, H. J. (1979), *Phys. Rev. D* **19**, 2320.  
 Peccei, R. D. and Quinn, H. (1977), *Phys. Rev. Lett.* **38**, 1440.  
 Rigby, K. W., Marek, D., and Chui, T. C. P. (1990), *Rev. Sci. Instr.* **2**, 834.  
 Turner, M. S. (1990), *Phys. Rep.* **197**, 67.  
 Weinberg, S. (1978), *Phys. Rev. Lett.* **40**, 223.  
 Wilczek, F. (1978), *Phys. Rev. Lett.* **40**, 279.